Dispersion Effects in Optical Millimeter-Wave Systems Using Self-Heterodyne Method for Transport and Generation

Rolf Hofstetter, Harald Schmuck, and Rolf Heidemann

***Abstract*—This paper describes the detrimental effects of chromatic and polarization mode dispersion (PMD) on systems using single-laser-based optical self-heterodyning for generation and transport of millimeter (mm)-wave signals. The decrease of the generated mm-wave power due to chromatic dispersion in conjunction with nonnegligible laser phase noise is calculated and experimentally verified. Considering statistical properties of the PMD an analytical expression for the cumulative probability distribution of the power penalty is found and used to determine the required system margin for a given system outage rate. Furthermore, two system experiments using ASK and DPSK modulation scheme, respectively, are presented showing no limitation due to the dispersion effects.**

I. Introduction

WIRELESS access to broadband networks providing high data rate flows to the user have to operate in the mm-wave ranges. The frequency bands around 30 and 60 GHz offer reaonable bandwidth and hence are now being, or will be, allocated for applications like asymmetric interactive multimedia services (IMS), broadband mobile services (MBS), and uni-directional distribution services for traffic information in intelligent vehicle highway systems (IVHS). At these frequencies the usage of a network architecture with micro and pico cells is mandatory in order to serve large areas with radio access. Fig. 1 shows the typical architecture of a 30/60-GHz fiber-optic broadcasting system. The main problem to be solved for such high capacity information systems is to transport mm-wave signals between one central station and many remote antenna units (RAU). Due to the large bandwidth and the low attenuation, fiber-optic technology appears to be a good candidate to solve this problem. It allows to concentrate and share equipment at a central site and to use remote antennas with low complexity.

The design of optical systems for this kind of application is not straightforward. Today, direct modulated lasers have bandwidths up to 25 GHz. Using external modulators the modulation bandwidth of an optical system can be extended to 75 GHz since mm-wave optical modulators and p-i-n photodiodes up to this frequency are available. But there are several detrimental effects:

1) Attenuation of the optical signals due to fiber attenuation and optical splitting makes the application of optical amplifiers mandatory for large networks. This confines the operating wavelength to the 1530–1560 nm gain window of erbium-doped fiber amplifiers.
2) The re-use of existing standard fiber links with chromatic dispersion $D = 17$ ps/(nm·km) at $\lambda = 1550$ nm strongly limits the link length. Due to the different propagation times of the contributing spectral components, the resulting mm-wave power will be degradated. For example, even with ideal external optical modulators operating at a modulation frequency of 30 GHz, the mm-wave power vanish after a fiber link length of 2.2 km.
3) Fiber nonlinearities are limiting the maximum optical power within the fiber. Stimulated Brillouin scattering, especially, can be a severe limiting factor if techniques are adopted that require narrow linewidth optical sources.

Several different approaches for optical generation and distribution of mm-wave signals have been proposed, e.g., in [1]–[3]. In order to cope with the limiting dispersion effects, optical self-heterodyne techniques [4]—as well as other remote heterodyne coherent schemes using e.g., phase locking of laser signals [5], [6]—should be applied.

In this paper we investigate detrimental dispersion effects in optical mm-wave systems that use self-heterodyne method for transport and generation. A single-laser scheme is presented that uses double sideband modulation with suppressed carrier [7] at half the mm-wave frequency (e.g. 15 GHz for 30-GHz transmit frequency) of a conventional distribution feedback laser [8], [9]. Theoretical and experimental results of system degradation due to chromatic- and polarization-dispersion effects will be given.

II. The Self-Heterodyne Method

The block diagram depicted in Fig. 2 presents the principle setup of the mm-wave link including the dual frequency optical source providing two optical carriers separated by the desired mm-wave frequency.

Manuscript received January 15, 1995; revised April 6, 1995. This work was supported in part by the European Community, RACE-project R2005 "MODAL" (Microwave Optical Duplex Antenna Link).

The authors are with Alcatel SEL AG Research Center, 70430 Stuttgart, Germany.

IEEE Log Number 9413694.

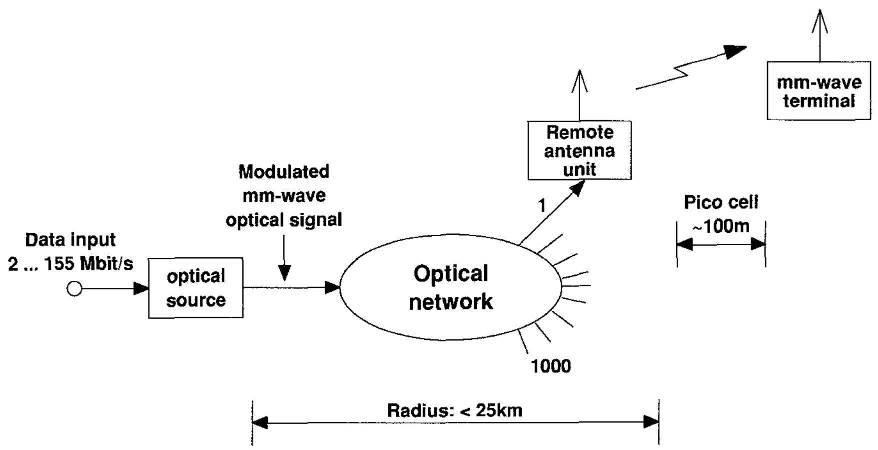

Fig. 1. Architecture of a 30/60-GHz fiber-optic distribution system.

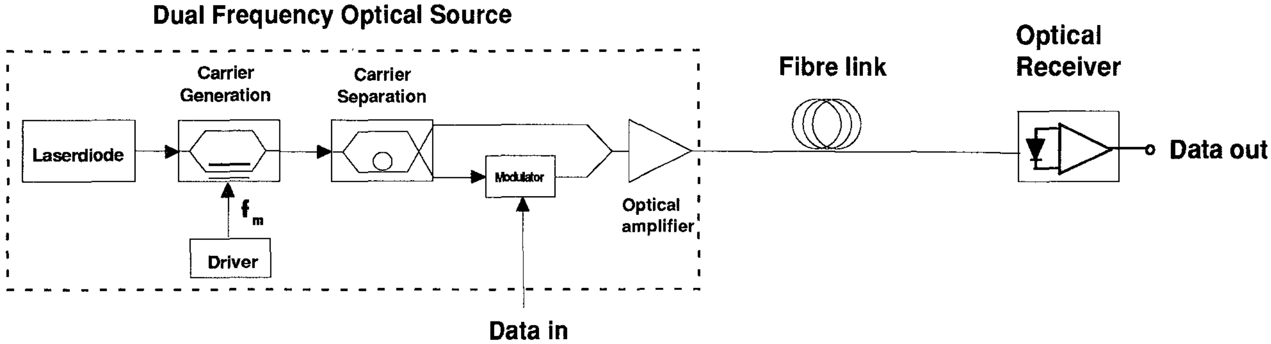

Fig. 2. Principle setup of optical mm-wave link.

The output signal of a laser diode emitting at a frequency ν_o is modulated by a CW-signal with an amplitude d_m and with a frequency f_m using a lithium niobate Mach-Zehnder modulator biased at U_b. Therefore, the output signal of the modulator results to

$$E(t) = \cos\left[\beta \cdot \frac{\pi}{2} + \alpha \cdot \frac{\pi}{2} \cdot \cos(\omega_M t)\right] \cdot \cos(\omega_0 t) \quad (1)$$

where $\beta = (U_b/V_\pi)$ is the normalized bias point of the modulator, $\alpha (= d_m/V_\pi)$ is the normalized amplitude of the drive signal, $\omega_m = 2\pi f_m$ is the modulation angular frequency, and $\omega_0 = 2\pi\nu_o$ is the angular frequency of the optical carrier. Using Bessel functions this equation can be expanded to

$$\begin{aligned} E(t) = {} & J_0\left(\alpha \cdot \frac{\pi}{2}\right) \cdot \cos\left(\beta \cdot \frac{\pi}{2}\right) \cdot \cos(\omega_0 t) \\ & - J_1\left(\alpha \cdot \frac{\pi}{2}\right) \cdot \sin\left(\beta \cdot \frac{\pi}{2}\right) \\ & \times \{\cos[(\omega_0 - \omega_m)t] + \cos[(\omega_0 + \omega_m)t]\} \\ & - J_2\left(\alpha \cdot \frac{\pi}{2}\right) \cdot \cos\left(\beta \cdot \frac{\pi}{2}\right) \\ & \times \{\cos[(\omega_0 - 2\omega_m)t] + \cos[(\omega_0 + 2\omega_m)t]\} + \cdots . \end{aligned} \quad (2)$$

For $\beta = 1$ (i.e. $U_b = V\pi$) all even terms vanish. In order to generate two strong carriers next to the optical center frequency ν_o with frequency difference $\Delta f = 2f_m$ (i.e. adopting optical amplitude modulation with suppressed carrier) the drive signal level has to be adjusted. An optimum operation point can be achieved by applying a drive signal level of $d_m \cong 1.2V_\pi$ corresponding to a normalized modulation amplitude of $\alpha = 1.2$. Here, the conversion loss of optical power due to the modulation is smaller than 1.6 dB (without considering insertion loss). In experiment the insertion loss have been measured to be 2 dB.

For data modulation the two optical carriers are separated by use of a fiber-optic Mach-Zehnder interferometer (MZI) filter. The fiber delay of the MZI and the frequency difference Δf have to be matched in order to realize a rejection of the unwanted optical carrier. One of the optical carrier is modulated by sub-carrier data signal(s) using a second amplitude modulator biased at V_π. Both optical carriers are combined and the optical power level is increased by an erbium-doped fiber amplifier. After transport over a fiber to the remote antenna side the coherent mixing of the carriers generates the mm-wave signal at frequency Δf. The signal is amplified and radiated into the micro/pico cells.

Due to the applied self-heterodyne technique the mm-wave show a high spectral purity. Measurements indicate spectral linewidths smaller than 100 Hz, which are limited by the spectrum analyser resolution bandwidth.

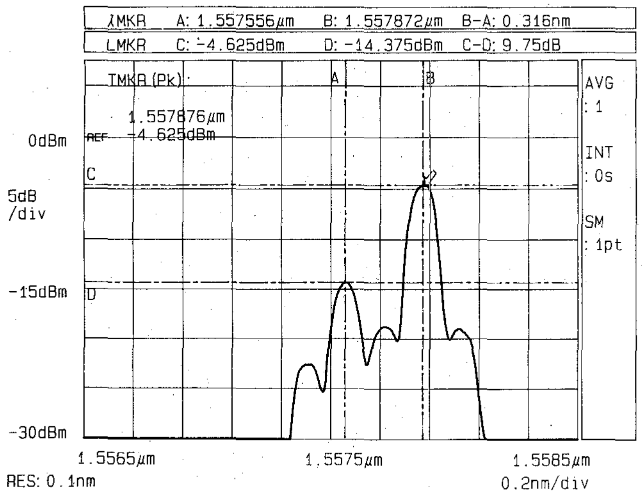

Fig. 3. Optical spectrum in front of the p-i-n photodiode. Vertical scale: 5 dB/div., horizontal scale: 0.2 nm/div., resolution bandwidth: 0.1 nm.

A typical optical spectrum in front of the broadband p-i-n photodiode is shown in Fig. 3. The wavelength separation of the two carriers is about 0.3 nm according to a frequency difference of $\Delta f = 30$ GHz. Here, a drive signal of $d_m = 21.8$ dBm ($\approx 1.2 V_\pi$) has been applied. The suppression of the original optical carrier with respect to the larger side-band carrier is better than 14 dB. The different power levels of the two sideband carriers are given by the additional attenuation of the second amplitude modulator (here: 4.8 dB) as well as by the choosen data modulation scheme (5 dB). Here, for data transmission a sub-carrier at 1.5 GHz has been applied. This modulation concept avoids that the information carrying mm-wave signals can interfere with other nonnegligible signal components.

III. Dispersion Effects

In this chapter theoretical and experimental investigations are presented that document the impact of the dispersion effects in the mm-wave fiber link. The properties of the mm-wave signal and the possible limitation due to the link have been investigated by use of the experimental set-up shown in Fig. 2. At the optical source two carriers separated by 30 GHz have been generated. The two signals are amplified and launched in a single-mode fiber. At the optical receiver within a commercial available broadband operating ($f_g = 40$ GHz) p-i-n photodiode the heterodyne process generates the mm-wave signal. After down conversion the spectrum of the signal is analysed. Here, no data transmission signal is applied.

A. Chromatic Dispersion

Because both optical carriers separated by the frequency difference Δf are generated from one single laser with nondisappearing linewidth $\Delta\nu$, their phase noise is completely correlated. Therefore, there is no broadening of the electrical carrier due to the phase noise of the original laser source. A propagation delay between the optical carriers caused by chromatic dispersion at the fiber will mean that at the p-i-n diode the phases of the two optical carriers are not completely correlated, which will lead to a linewidth broadening of the electrical mm-wave carrier—resulting in a peak power degradation.

As shown in [10] the total power at the pin photodiode is given by

$$P_D \propto 1 + \cos\{[\omega_0 \tau + 2\pi \Delta f(\tau - t)] + \Phi(t) - \Phi(t - \tau)\} \quad (3)$$

where τ represents a time delay for both optical carriers separated by a frequency offset of Δf and ϕ the rleative optical phase, respectively.

By calculating the autocorrelation function the power spectral density can be expressed as [10], [11]

$$\begin{aligned} S(\nu, \tau) \propto & \frac{\tau_C}{1 + \Delta\omega^2 \cdot \tau_C^2} \\ & \times \left\{ 1 - e^{-\frac{|\tau|}{\tau_C}} \cdot \left[\cos(\Delta\omega \cdot |\tau|) + \frac{\sin(\Delta \cdot |\tau|)}{\Delta\omega \cdot \tau_C} \right] \right\} \\ & + \pi \cdot e^{-\frac{|\tau|}{\tau_C}} \cdot \delta(\Delta\omega) \end{aligned} \quad (4)$$

with $\Delta\omega = 2\pi \cdot (\nu \pm \Delta f)$.

This result indicates that for a given coherence time $\tau_C = \frac{1}{2\pi \cdot \Delta\nu}$, the signal strength shifts from a delta function peak (representing the case when both optical carriers are totally correlated) more and more to a pure Lorentzian shape when both carriers are completely decorrelated.

For $\tau \ll \tau_c$ (i.e. for a low amount of dispersion induced phase noise) and a data rate $B_R \ll \frac{1}{\tau}$, the resulting phase noise can be further reduced by IF filtering [12]. In this case the system power penalty is mainly given by the mm-wave power degradation [last term in (4)], which leads to an increased bit-error rate (BER).

Standard single-mode fibers show a chromatic dispersion of typical $D = 17 \frac{\text{ps}}{\text{nm} \cdot \text{km}}$ at an operation wavelength of 1.55 μm. The theory introduced above show that by use of high performance laser ($\Delta\nu = 1$ MHz) as well as by commercially available laser ($\Delta\nu = 20$ MHz) the fiber dispersion effect is negligible small. For a 30-GHz mm-wave signal transmitting through a fiber link length of 100 km the chromatic dispersion will lead to a propagation time delay of 0.41 ns, which will result in a negligible carrier power degradation of below than 0.25 dB.

B. Phase Noise Induced by Fiber Delay

In the optical source a further decorrelation-inducing effect can appear: For data modulation the two optical carrier will be separated. After modulation of one carrier both signals are recombined. Therefore, the two carriers are transmitted in different fiber links with a propagation delay inducing a decorrelation comparable to the chromatic dispersion effect. In order to quantify the impact of this delay the power degradation in dependence on a propagation delay τ has been measured. Therefore, several pigtailed fiber jumper with a length up to 12 m (representing a time delay $\tau = 60$ ns) has been connected in order to simulate different fiber delays ΔL at the carrier separation unit (see Fig. 2). In Fig. 4 the experimental results as well as the theoretical curves calculated

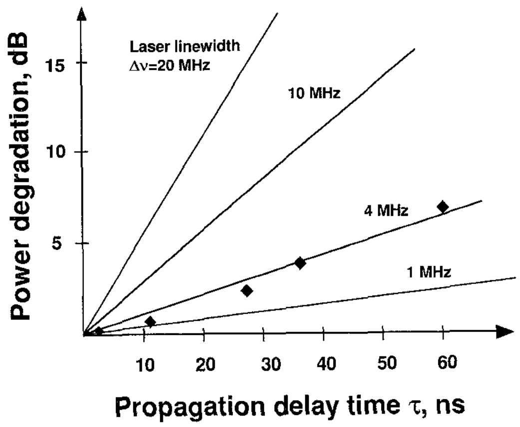

Fig. 4. Power degradation of 30-GHz mm-wave signal due to decorrelation of optical carrier in dependence of propagation delay time τ for different laser linewidths (theory: ——; experiment: □).

with (4) are shown. The experimental data are in a good agreement with the laser linewidth of the master laser, which is measured to be in the range of $\Delta\nu = 4$ MHz. In praxis in the optical source a fiber delay length difference of $\Delta L = 0.05$ m will be adjustable, which will result in a power degradation ΔP smaller than 0.15 dB.

C. Polarization-Mode Dispersion

It is well known that PMD can be a limiting factor in high speed, long haul fiber optical communication systems [13], [14]. Especially in systems where the chromatic dispersion at the fiber becomes very small, PMD effects can be observed because of a difference between the propagation delay times of the two polarization modes in a fiber exist.

Basicially, by the applied technique for optical generation of mm-wave signals at the photodiode the electrical power of the mm-wave signal depends on the state of polarization of the two field components with respect to each other. Due to PMD in the fiber given by the differential group delay $\Delta\tau$ the two optical carriers have different states of polarization at the pin diode. The polarization mismatch induces a power degradation of the mm-wave signal at the receiver, which leads to an increase of the BER.

In [15] for the first time experimental and theoretical results concerning the influence of polarization-mode dispersion (PMD) in an advanced fiber-optic supported mm-wave system have been presented. A theoretical approach for calculation the power penalty due to PMD has been confirmed by experimental results at 60 GHz using a high-birefrigence single-mode fiber (PANDA-type) showing an extremely high PMD effect.

Based on [15] and considering the general case it can be shown that the power penalty ΔP due to a PMD $\Delta\tau$ at the fiber link is given by

$$\Delta P(L, \gamma, \Delta\tau) = -10 \cdot \log \left[\frac{1 + f(\gamma) + \cos^2(k(\Delta\tau)) \cdot (1 - f(\gamma))}{2} \right] \quad \text{for } \Delta\tau \geq 0, L \geq 0, \; 0 \leq \gamma \leq 1 \tag{5}$$

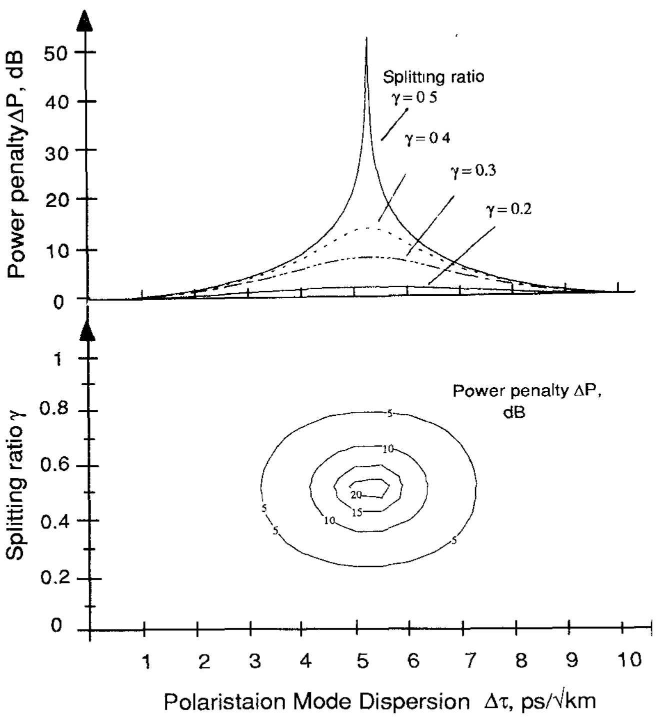

Fig. 5. Power penalty ΔP at 30 GHz mm-wave signal due to PMD $\Delta\tau$ in a 10-km-long single-mode fiber in dependence of power splitting γ (upper traces) and the corresponding level diagramm of power penalty ΔP (lower traces).

with $f(\gamma) = \cos[4 \cdot \arccos(\sqrt{\gamma})]$, $k(\Delta\tau, L) = \pi \cdot \Delta f \cdot \Delta\tau \cdot L$, L the fiber link length and $\Delta\tau$ the actual value of PMD. The parameter γ represents the power splitting ratio of the signal light at the fiber link input port with respect to the prinzipal axes.

In Fig. 5 the power penalty ΔP for a mm-wave signal at $\Delta f = 30$ GHz in dependence of the PMD value $\Delta\tau$ of the fiber ($L = 10$ km) and the splitting factor γ is shown. For $\gamma = 0.5$ the worst case of power penalty exists. Here, at a PMD of

$$\Delta\tau = \frac{m}{2 \cdot \Delta f} \qquad (m = 1, 3, 5, \ldots) \tag{6}$$

the mm-wave power vanishes, representing the case when both optical fields are in a state of polarization orthogonal to each other.

At realistic transmission systems in long standard single-mode fibers (e.g. full installed submarine or terrestrial cable) the PMD value varies randomly with time and wavelength. For example, temperature effects cause changes in the actual birefrigence in the fiber, which results in random polarization mode coupling. Therefore, a more detailed analysis of the impact of PMD in the mm-wave system should consider the statistical variation of the PMD values.

The statistics of the actual PMD value $\Delta\tau$ [16] varies with a Maxwellian probability distribution function

$$M(\Delta\tau, \Delta\tau_M) = \frac{32 \cdot \Delta\tau^2}{\pi^2 \cdot \Delta\tau_M^3} e^{\left(-\frac{4}{\pi}\left(\frac{\Delta\tau}{\Delta\tau_M}\right)^2\right)} \tag{7}$$

which is determined by mean value $\Delta\tau_M$.

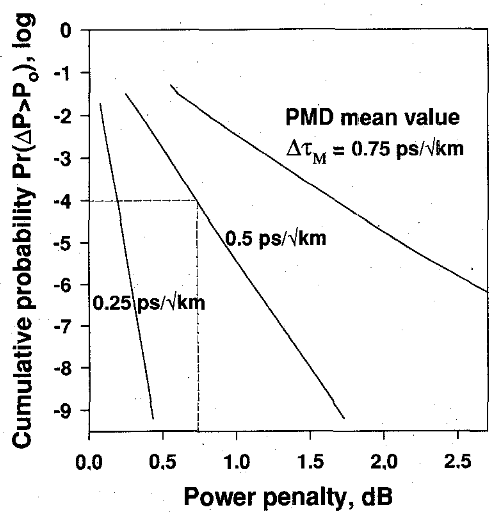

Fig. 6. Cumulative probability Pr to get power penalty $\Delta P > P_o$ for different PMD mean values $\Delta\tau_M$. Millimeter-wave frequency: 30 GHz; fiber link length: 10 km.

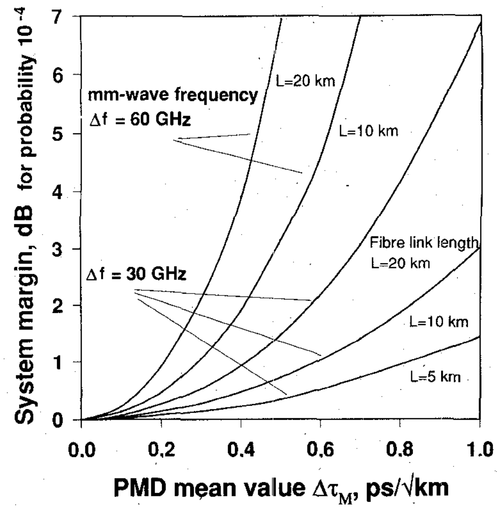

Fig. 7. System margin calculated for the probability Pr $= 10^{-4}$ in dependence of PMD mean value $\Delta\tau_M$ and fiber link length L. Millimeter-wave frequency: 30/60 GHz.

Furthermore, there are random variations of the actual angle of incident of the linear polarized lightwaves launched into the fiber link with respect of the fiber main axes. This effect can be described by an uniform probability distribution of power splitting γ in the main axes.

As shown in the lower traces of Fig. 5 the parameter $\Delta\tau$ and γ span a plane for the power degradation, which can be used in order to calculate the cumulative probability

$$\begin{aligned}\Pr(\Delta P \geq P_0) &= \int\int M(\tau', \Delta\tau_M)d\tau' \cdot d\gamma \\ \Delta P(L, \tau', \gamma) &\geq P_0. \end{aligned} \quad (8)$$

$\Pr(\Delta P > P_0)$ represent a mm-wave system quality parameter that describes the probability of getting a penalty larger than P_0 in dependence of the fiber length L and the given PMD mean value $\Delta\tau_M$, respectively.

In Fig. 6 the cumulative probability in dependence on several PMD mean values are shown. For our calculations we assume a fiber link length of 10 km, which will be sufficient for future mm-wave systems, like, e.g., information distribution systems. $\Delta\tau_M$ vary between moderate values of 0.25 ps/$\sqrt{\text{km}}$ up to high values of 0.75 ps/$\sqrt{\text{km}}$. For full installed fiber cables PMD values smaller than 0.5 ps/$\sqrt{\text{km}}$ can be expected.

For the design of radio links operating at 30 GHz, with, e.g. outage due to rain fading, a system availability of 99.99% (prob $= 10^{-4}$) is sufficient, representing an outage up to 1 hour per year. With the same probability a power penalty larger than 0.74 dB caused by a fiber with a PMD mean value of $\Delta\tau_M =$ 0.5 ps/$\sqrt{\text{km}}$ can be expected.

Based on the considerations in Fig. 7, the system margin needed to compensate for the PMD effects in future fiber supported mm-wave systems are depicted for mm-wave frequencies of 30 and 60 GHz, respectively. The overall results of these theoretical investigations will be that for mm-wave frequencies up to 60 GHz region and for fiber links showing moderate mean values up to fiber length of 20 km the PMD in fiber-supported mm-wave systems leads to an acceptable power penalty of $\Delta P < 2$ dB.

IV. Applications

The potential application area of the fiber-optic mm-wave technology in broadcasting high capacity information at any desired mm-wave frequency up to >100 GHz has been demonstrated with a feasibility experiment [17]. The building blocks are shown in Fig. 8. The self-heterodyne method for generation and transport enabled to distribute a 36 GHz–140 Mbt/s-DPSK modulated mm-wave signal over a fiber link of 25 km to more than 16 000 base-stations. After free-space transmission, demodulation, and detection neither degradation nor limitation due to dispersion has been observed down to BER of 10^{-9}.

In order to demonstrate the performance of the used self-heterodyne method for bi-directional applications, a full duplex mm-wave transmission experiment has been (Fig. 9) carried out within the RACE project R2005 MODAL An optical 30-GHz mm-wave link at a wavelength of 1550 nm has been extended by an optical 1.8-GHz microwave return path operating at 1300 nm. At the central station one of the two optical carriers with frequency difference of 30 GHz is amplitude modulated by a 1.5-GHz-2 Mbt/s-ASK subcarrier signal. After transmission over a 12-km-long single-mode fiber the signals mix on the p-i-n photodiode and generate a mm-wave carrier together with sidebands that correspond to the modulating subcarrier at the base station. An amplifier integrated with the p-i-n photodiode is followed by a diplexer that allow separate selection of one of the sidebands and of the unmodulated 30-GHz mm-wave carrier. The selected sideband (31.5 GHz) is amplified and radiated using a horn antenna.

After free-space transmission, a transposer is used in order to down convert the 31.5 GHz to 28.2 GHz. The resulting return signal from the transposer, which is received by a

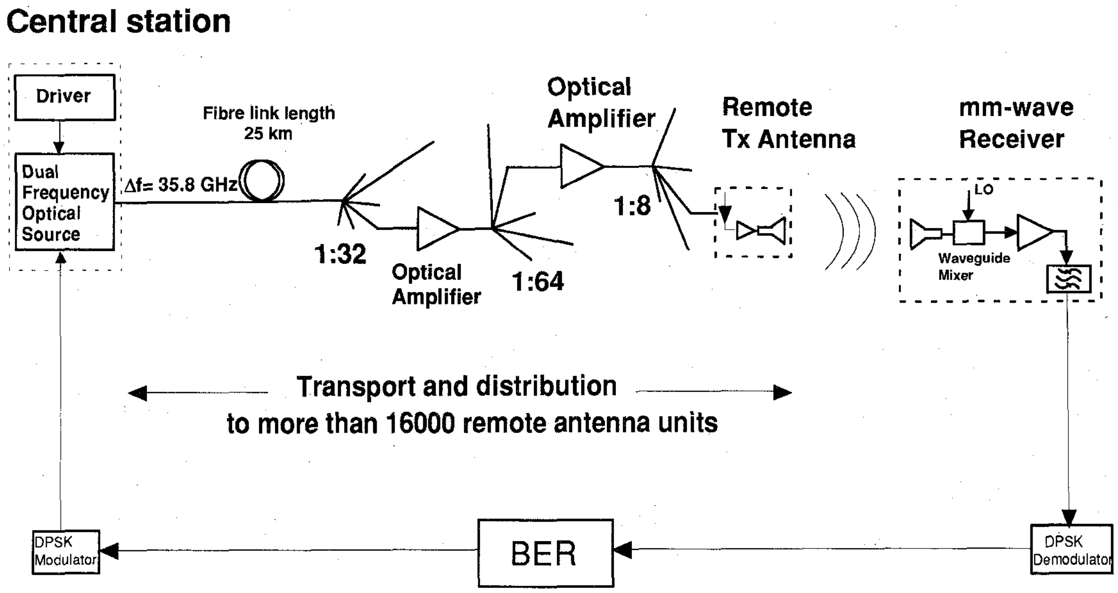

Fig. 8. Block diagram of 140 Mbt/s transmission experiment at 36 GHz.

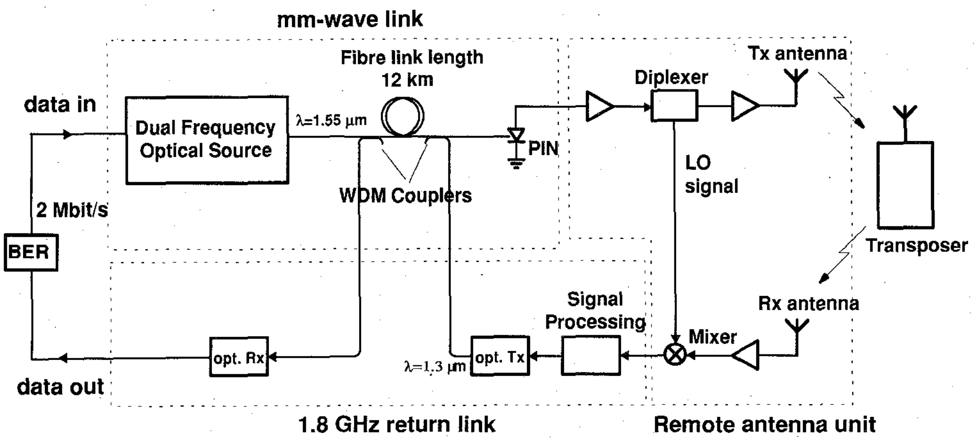

Fig. 9. Topology of the MODAL demonstrator.

separate Rx antenna, is amplified and mixed with the recovered 30-GHz carrier in order to downconvert it to 1.8 GHz. This IF signal is amplified and used to modulate the laser of the return link. The same fiber as used for down transmission supports the return link to the base station by means of WDM couplers. The result of a bit-error-rate (BER) measurement indicates that there is no BER-floor due to dispersion effects down to 10^{-7}.

V. Conclusion

The impact of detrimental effects due to chromatic dispersion and polarization-mode dispersion (PMD) on systems applying the self-heterodyne method for generation and transport of mm-wave signals has been investigated. The power degradation due to the chromatic dispersion in conjunction with non negligible phase noise of the optical carriers was found to be moderate low (¡0.5 dB) for high capacity long haul mm-wave systems (140 Mbt/s, 100 km).

It is shown that PMD has a significant effect on the system performance. Based on the statistical behavior of the resulting polarization states at the output of the fiber, an analytical expression has been derived for the cumulative probability function of the resulting power penalty. It was found that for a permissible outage time of less than 1 hour per year and a fiber length of $L = 20$ km, a system margin of 2 dB is sufficent for a mean PMD of 0.25 ps$\sqrt{\text{km}}$. Finally, two system experiments have been presented using ASK and DPSK modulation schemes. Here, no limitation due to the dispersion effects could be observed.

References

[1] A. J. Cooper, "Fiber/radio for the provision of cordless/mobile telephony services in the access network," *Electron. Lett.*, vol. 26, pp. 2054–2056, 1990.

[2] A. J. Seeds and A. A. A. de Salles, "Optical control of microwave semiconductor devices," *IEEE Trans. Microwave Theory Tech.*, vol. 38, pp. 577–585, 1990.

[3] S. Kawanishi, A. Takada, and M. Saruwatari, "Wide-band frequency response measurement of optical receiver using optical heterodyne detection," *J. Lightwave Technol.*, vol. 781, pp. 92–98, 1988.
[4] M. J. Wale, R. G. Walker, and C. Edge, "Single-sideband modulator in GaAs integrated optics for microwave frequency operation," Integrated Photonics Research, *OSA Tech. Dig. Ser.*, vol. 10, post-deadline paper PD-8, 1992.
[5] U. Gliese *et al.*, "A wideband heterodyne optical phase-locked loop for generation of 3–18 GHz microwave carriers," *IEEE Photon. Technol. Lett.*, vol. 4, pp. 936–938, 1992.
[6] P. Gallion *et al.*, "Single-frequency laser-phase noise limitation in single-mode optical-fiber coherent detection systems with correlated fields," *J. Opt. Soc. Am.*, vol. 72, no. 9, pp. 1167–1170, 1982.
[7] M. Izutsu, S. Shikama, and T. Sueta, "Integrated optical SSB modulator/frequency shifter," *IEEE J. Quantum Electron.*, vol. QE-17, no. 11, pp. 2225–2227, 1981.
[8] J. J. O'Reilly, P. M. Lane, R. Heidemann, and R. Hofstetter, "Optical generation of very narrow linewidth millimeter wave signals," *Electron. Lett.*, vol. 28, pp. 2309–2311, 1992.
[9] R. Heidemann and R. Hofstetter, "A novel optical mm-wave generation and transport system," in *Proc. MIOP '93, 7th Exhibition and Conf. for Ultra High Frequency Technology*, Sindelfingen, Germany, May 25–27, 1993, pp. 251–254.
[10] L. E. Richter, H. I. Mandelberg, M. S. Kruger, and P. A. McGrath, "Linewidth determination from self-heterodyne measurements with subcoherence delay times," *IEEE J. Quantum Electron.*, vol. QE-22, no. 11, pp. 2070–2074, 1986.
[11] L. Goldberg, R. D. Esman, and K. J. Williams, "Generation and control of microwave signals by optical techniques," *IEE Proc.*, pt. J, vol. 139, no. 4, pp. 288–295, 1992.
[12] U. Gliese, E. L. Christensen, and K. E. Stubkjaer, "Laser linewidth requirements and improvements for coherent optical beam forming networks in satellites," *J. Lightwave Technol.*, vol. 9, pp. 779–789, 1991.
[13] E. Iannone, F. Matera, A. Galtarossa, G. Gianello, and M. Schiano, "Effect of polarization disperison on the performanceof IM-DD communication systems," *IEEE Photon. Technol. Lett.*, vol. 5, pp. 1247–1249, 1993.
[14] H. Bülow, "Operation of a digital optical transmisson system with minimal degradation due to polarization mode dispersion (PMD)," *Electron. Lett.*, vol. 3, pp. 214–215, 1995.
[15] H. Schmuck, "Effect of polarization-mode dispersion in fiber-optic millimeter-wave systems," *Electron. Lett.*, vol. 18, pp. 1503–1504, 1994.
[16] A. Galtarossa *et al.*, "Polarisation mode dispersion in long single-mode-fiber links: A review," *Fiber and Integrated Optics*, vol. 13, pp. 215–229.
[17] H. Schmuck, R. Hofstetter, and R. Heidemann, "Advanced fiber-optic distribution of 140 Mbit/s mm-wave signals at 36 GHz," in *20th European Conf. on Optical Communication ECOC '94*, Florenz, Sept. 1994, pp. 25–29.

Rolf Hofstetter received the Dipl. Ing. degree from HTL in Rapperswil (1979), the Dipl. El. Ing. degree (1983), and the Dr. sc. techn. degree (1990) from ETH in Zurich, Switzerland.

From 1984–1991 he was Research Assistant of the Communication Technology Laboratory, ET Zurich. He was with the Alcatel SEL Research Center from May 1991–March 1995. There, he was responsible for the project management of RACE R2005 MODAL. Within this project he investigated the linearization and application of low cost optical links for PCN and the optical transport and generation of mm-wave signals. Since April 1995 he has been Professor of Transmission Systems at the Engineer School HTL Chur. His technical areas of experience are communication systems and optical microwave and mm-wave transmission.

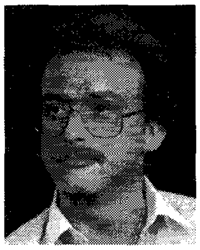

Harald Schmuck received the Diplom degree in physics from the University of Kaiserslautern, Germany, in 1983. His research work included fiber-gyro technology.

He then joined the Alcatel SEL Research Center, Stuttgart, and was engaged in the field of fiber-optics in sensors and coherent transmission technique. His primary areas of work have been optical transmission technology and fiber-optic components, like optical filters and erbium fiber ring lasers. Presently he is involved in the development of optical microwave and mm-wave transmission technique.

Rolf Heidemann received the Diplom Physicist degree and the Dr. rer. nat. degree in 1976 and 1983, respectively, from the Institute of Applied Physiks, University of Münster, Germany.

From 1978 to 1983 he was a Research Assistant at the Institute of Applied Physics. He joined the Alcatel SEL Research Center in 1983 and became Head of the Fiber-Optics Transmission Department in 1985. His technical areas include subscriber line systems (B-ISDN), analogue and digital fiber-optic CATV systems, multigigabit/s transmission systems, and photonic technologies (optical amplification, regeneration, switching, soliton transmission).